DEVELOPMENT OF A HIGHLY DETAILED NUMERICAL MODEL OF FOAM CORE SANDWICH PANEL SUBJECTED TO MMOD IMPACT

Victor O. Babarinde [(1)], Anton Kuznetcov [(1)], Igor Telichev[(1)]

[(1)] Department of Mechanical Engineering, University of Manitoba, E2-327 EITC, 75A Chancellors Circle, Winnipeg, Manitoba, R3T 5V6, Canada, Email: babarinv@myumanitoba.ca

ABSTRACT

Research conducted in the past decade on aluminum open-cell foam demonstrated its effectiveness for space application. The present study is focused on the development of the numerical model of foam using the Weaire-Phelan structure.

The geometrical features of the physical foam, such as ligament lengths and diameters and diameters of nodes at ligaments' intersections, were used to generate the highly detailed numerical model of foam.

The developed numerical model was applied to simulate the hypervelocity impact of 6-mm MMOD particles on the sandwich panel with an open-cell aluminum foam core. The obtained numerical results were found to be in good agreement with test data.

1 INTRODUCTION

The presence of non-ballistic components in the design of the conventional shields affects their weight efficiency. Studies [1-5] performed during the past decade demonstrated that multi-functional sandwich panels with the open-cell aluminum foam offer an adequate level of protection against micrometeoroids and orbital debris (MMOD) without the need for the parasitic mounting elements.

In addition to the experimental studies on the efficiency of aluminum foam for MMOD protection of spacecraft, a numerical simulation is essential for a complete understanding of how the foam characteristics affect the fragmentation process.

Various methods have been established to model different foam structures numerically, including the Voronoi Tessellation, Laguerre-Voronoi Tessellation, Poisson-Voronoi Tessellation, Kelvin unit cell, and Weaire-Phelan unit structure.

The Voronoi, Laguerre-Voronoi, and Poisson-Voronoi have been used to model the foam structure through a series of spatial tessellations [6-8]. These methods involve generating random points in space and creating space based on the closeness of points to one another. Since the Laguerre-Voronoi and Poisson-Voronoi are Monte-Carlo-based methods, the generated foam will not exactly be the same as the original physical foam but rather stochastic and representative on a mesoscale.

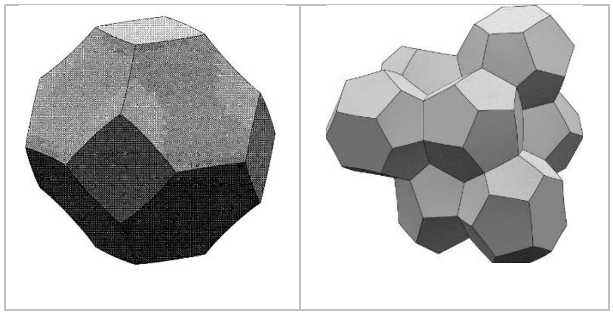

a) *b)*

Figure 1. (a) Kelvin unit model; (b) Weaire - Phelan unit model [14].

The Kelvin unit structure is constructed on a regular tetrakaidecahedra (fourteen faces) with eight hexagonal and six square faces (Fig. 1a), ensuring equal volume with minimal surface energy [9]. Though the pentagonal faces have been studied to be abundantly available in the realistic foam structure, the Kelvin structure lacks such faces. In pursuit of a more practical form model, the Kelvin structure was subjected to some criticisms, which are based on the anisotropic nature of the mechanical properties and insufficient randomness, which are essential characteristics of foam structure [10-13]. A better solution was found by Weaire and Phelan [14], which allows constructing a unit cell with lower surface energy than the Kelvin unit structure. The Weaire-Phelan foam unit contains an equal volume of six 14-sided cells (2 hexagonal and 12 pentagonal faces) and two 12-sided polyhedral (Fig. 1b).

The use of the Weaire-Phelan unit for the simulation of 40 pores per inch (PPI) foam subjected to hypervelocity impact (HVI) of 1-mm spherical aluminum projectile can be seen in a study [5] performed at the University of Manitoba. The result of the simulation showed an excellent correlation between the numerical and experimental results.

The approach introduced in [5] was used in the present study to expand it to simulate the impact of 6-mm particle vs 1-mm used in [5], which is 216 times larger by mass and volume. Another goal was to introduce the foam

manufacturing features and their stochastic distributions into the numerical model. Modelling also employed the enhanced randomization procedure, which involved perturbation of both the positions and the sizes of nodes and ligaments as well as random rotation of sub-units.

2 FOAM GEOMETRY MODELLING

2.1 Analysis of Geometrical Features

The geometry of the aluminum foam is studied in detail in a number of papers. The non-destructive studies (e.g. [10, 13, 15-17]) performed on the foam structure allowed scientists to get insight into the foam geometry. Obtained data like the ones shown in Fig. 2 serve as a valuable source of detailed information for developing the numerical model of foam [17].

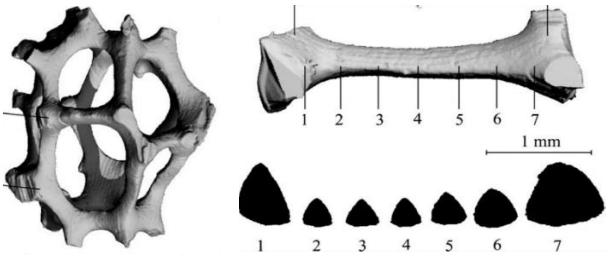

a) b)

Figure 2. Geometry of cells (a) and ligaments (b) for open-cell aluminum foam [17]

In the proposed numerical model, the geometry of the foam was created from simple geometric primitives such as cylinders and spheres. The cylinders represent the foam ligaments, while spheres represent the roots of the ligaments created at their intersections. A simple statistical analysis was performed on the aluminum 40 PPI foam sample supplied by the ERG Aerospace (Fig. 3a).

Nine cells were randomly selected on the surface of the sample, and for each cell (Fig. 3b), the following parameters were measured: 1) length of the ligaments (L); 2) mid-span diameter of the ligaments (DL); 3) diameters of the spheres at the ligament junction (DS).

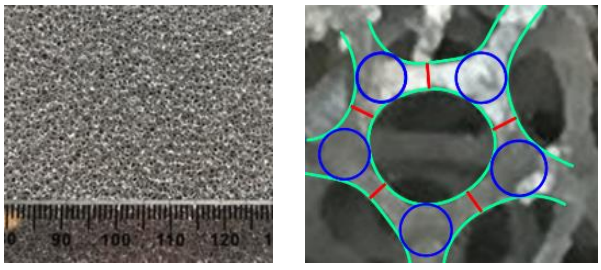

a) b)

Figure 3. 40 PPI foam from the ERG Aerospace (a) and randomly selected cell (b)

The results of the measurements are shown in the form of histograms and representative values in Fig. 4.

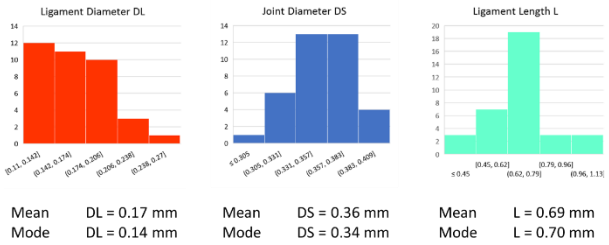

Figure 4. Distribution of 40 PPI foam parameters

2.2 Generation of Foam Structure

The overall approach uses the Weaire-Phelan (WP) unit scaled to achieve the target PPI based on the measured average ligament size (Fig. 5a). Then, the representative volume element (RVE) is generated using ANSYS Parametric Design Language (APDL) script, which was developed to concatenate the Weaire-Phelan foam unit into the wireframe structure of desired size (Fig. 5b).

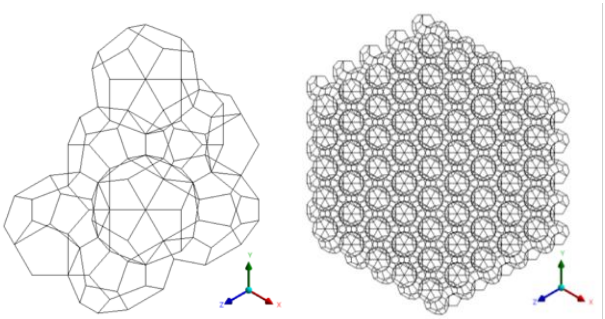

a) b)

Figure 5. Regular wireframe foam structure

Next, the obtained DL- and DS-distributions within the 95% confidence interval are applied to the variation of model foam's geometric parameters. In the 40 PPI 3% aluminum foam model (before the randomization was applied), the ligament length was equal to L=0.7 mm, and the ligament diameter and diameters of the spheres at the ligament junctions varied within the intervals DL=0.1307..0.1993 mm and DS=0.3252..0.3792 mm respectively. Tab. 1 illustrates the consistency of the numerical model geometry with physical foam and data from the literature.

In order to improve the conformity of the model with the physical foam, a randomization algorithm is run for the obtained wireframe, moving each node in a random direction by a small random value. Still, the degree of randomization in the foam model was not sufficient; thus, to improve on the randomization, the RVE was divided into smaller units, then each unit is randomly rotated within the range of ±90º (Fig. 6).

Table 1. Comparison of the ligament length

Source of data	Average ligament length *(L)*, mm		Ratio L_{20PPI}/L_{40PPI}
	20 PPI	40 PPI	
Ref. [17, 18]	1.22	1.04	1.173
Sample	0.809	0.690	1.172
Model	0.833	0.707	1.178

The resulting solid body is cut to the desired dimensions and shape. All individual bodies in the model are merged together by a Boolean operation. The final designs for the foam model are presented in Fig. 7 and 8.

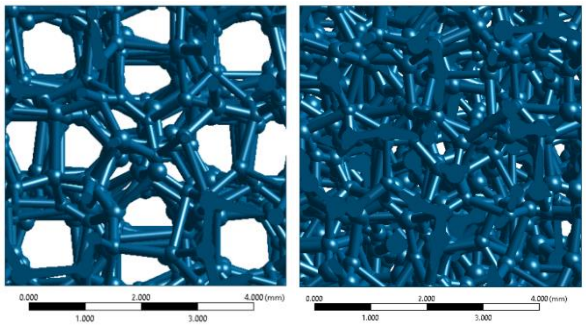

a) b)

Figure 6. Foam geometry after randomization: (a) 20 PPI 4.23% aluminium foam; (a) 40 PPI 7.45% aluminium foam

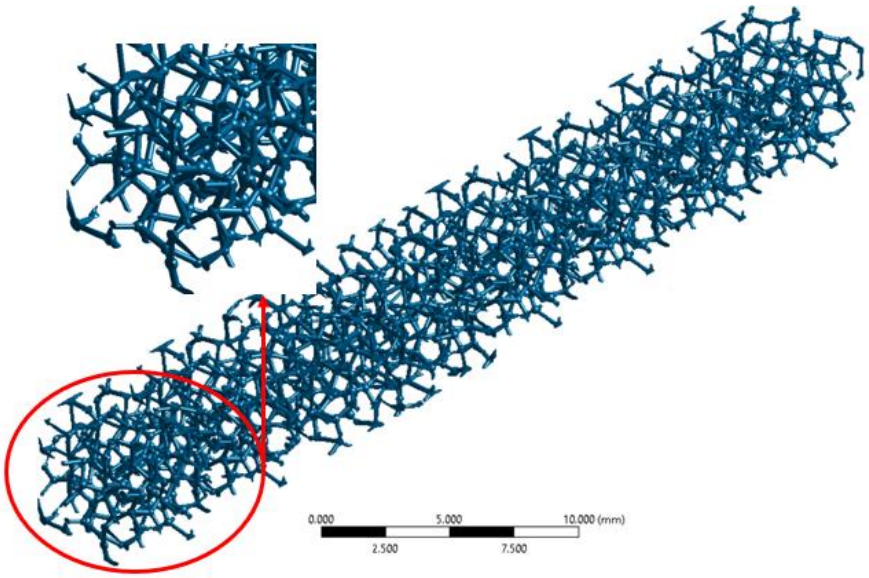

Figure 7. Model of 20 PPI 4.2% aluminum foam

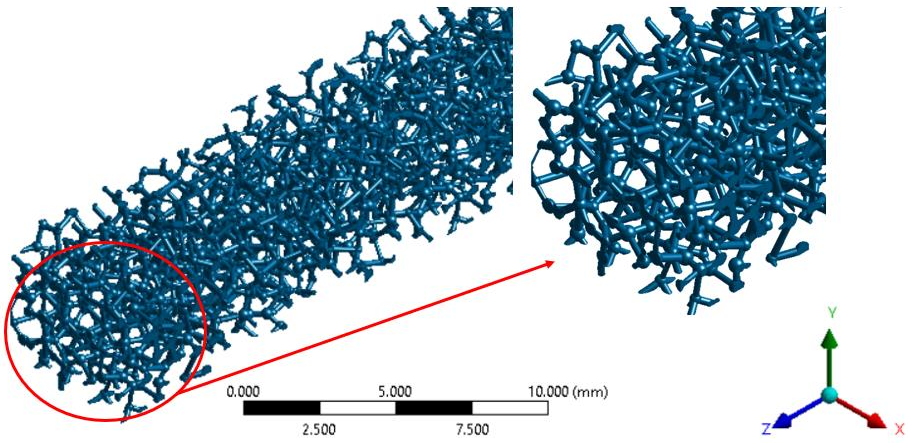

Figure 8. Model of 40 PPI 7.5% aluminum foam

3 NUMERICAL MODEL OF FOAM-CORE SANDWICH PANEL

3.1 Model Description and Parameters

The numerical model is developed to simulate the hypervelocity impact on the foam core sandwich panel (FCSP). The FCSP comprises two face sheets and an intermediate core made from an open-cell foam structure. All parts of the panel were fabricated from Al6061-T6. The details of the geometrical characteristics of the model are presented in Tab. 2 and Fig. 9. The t_f and t_r thicknesses of the facesheets were selected identical and varied with the range from 0.8 mm to 2.0 mm.

Table 2. FCSP Model parameters

FCSP	*S, mm*	*W, mm*	*H, mm*	d_p, *mm*
20 PPI	40.0	10.0	10.0	6.0
40 PPI	40.0	10.0	10.0	6.0

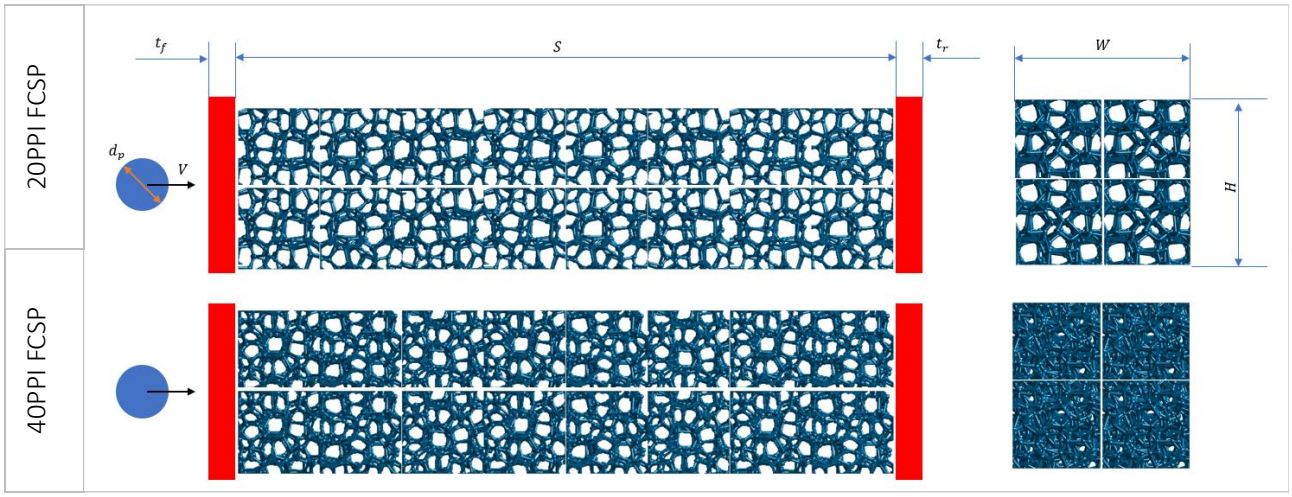

Figure 9. FCSP model parameters

3.2 Numerical Modelling Approach

The numerical simulation of an aluminum foam-core sandwich panel under hypervelocity impact involves a combination of different material states, extreme temperature, and excessive material distortion. In this study, the smoothed particle hydrodynamics (SPH) method and grid-based finite element method (FEM) in the Lagrangian formulation were combined into the numerical model of foam core sandwich panel subjected to the hypervelocity impact. The SPH was used to model the projectile's behaviour, front face sheet, and the foam core; this was due to the high deformation of the material and possibly a change of material state in these regions. The simulation was performed using ANSYS Autodyn. The numerical HVI test setup is shown in Fig. 10.

As the projectile fragments propagate through the panel, the shock wave intensity and deformation rate decrease, giving us the opportunity to use a grid-based approach. So, the impact response of the rear facesheet (or back wall) was modelled with the use of FEM alongside the implementation of the erosion algorithm. A quarter model was analyzed to reduce the computational cost, and the symmetry boundary condition was imposed in both y-z and x-z planes. Though the foam core has a random structure, the symmetry condition's decision was based on the foam's consistent porosity and the isotropic nature of its effective properties. It is important to note that this might not be the case if the Kelvin unit was used as the building block due to its anisotropic nature.

In Autodyn, the compatibility of both the grid-based FEM and the mesh-free SPH methods allows using the same constitutive laws without any modifications. The identical size of SPH was selected for all SPH parts within the FCSP model to avoid the numerical inconsistencies during transitioning from one particle size to another. This choice, however, makes the simulation computationally expensive due to the considerable difference in the dimensions of the foam ligaments and the facesheet thickness.

3.3 Material Models

Three models are required for the numerical modelling of the hypervelocity impact simulation of the FCSP: (1) the Equation of state (EOS), which gives the relationship between the local density, specific energy, and the hydrostatic pressure; (2) the strength model, which relates the deviatoric stress with the strain and temperature effect; and (3) the failure model, which

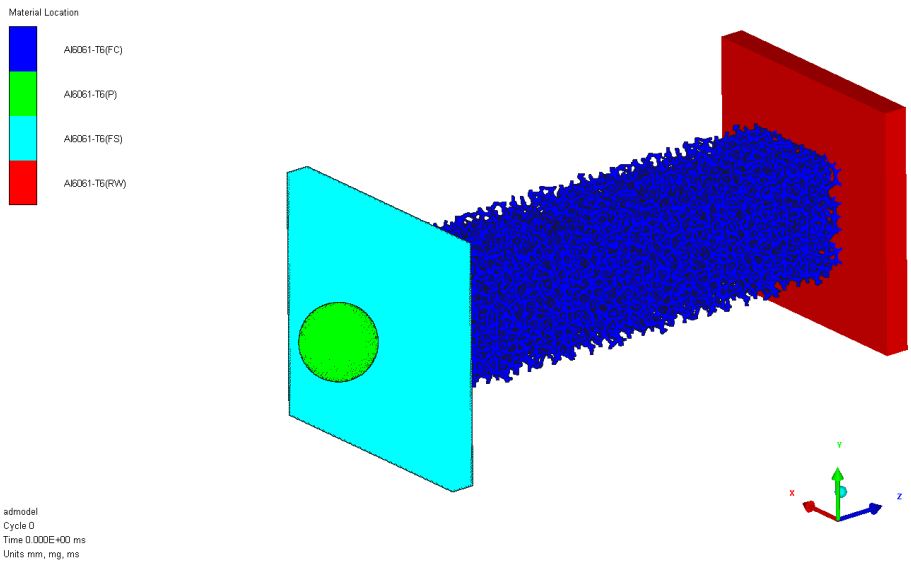

Figure 10. Numerical HVI test setup for 40 PPI foam core sandwich panel (FC-foam core; P - projectile; FS - front facesheet; RW - Rear wall)

represents the initiation of material failure in the model. In this study, the Mie-Gruneisen EOS, the Johnson-Cook (JC) strength and failure models were used due to the large deformation, elevated temperature, and the high strain rate involved in the hypervelocity simulation. The material model parameters for Al6061-T6 were selected to be identical to that of [5].

4 MODEL CALIBRATION

The developed numerical model employs FEM approach in the Lagrangian formulation for the sandwich panel's rear facesheet. Thus, erosion strain value (e) was needed to prevent excessive mesh distortion and mesh tangling in the rear wall. This is a non-physical parameter selected from the comparison of the physical test data and results of the calibration numerical experiments conducted for the erosion strain ranging from 0.7 to 1.3. The parameters of the HVI test setup (both numerical and physical) are presented in Tab. 3. To access the damage after the physical and numerical tests, the diameter of the perforated hole in the rear facesheet (D_h) and its maximum deflection (p) were determined and compared. The outcome of the physical HVI test is illustrated in Fig. 11.

The calibration study was conducted on the foam models implementing the following two approaches: a) "Constant" approach uses equal (average) values for all ligaments and nodes; b) "Stochastic" approach introduces a statistically justified level of randomness into the nodes and ligament sizes. The performed analysis showed that an erosion strain of 1.0 allows obtaining an acceptable prediction for the HVI test outcome. The selected e=1 is consistent with the conclusion made in [5] for the same material. The "Stochastic" approach with introduced stochastic variations of foam parameters gives a more accurate result (Fig. 12b) than the "Constant" approach (Fig. 12a).

Table 3. HVI test setup parameters

Projectile diameter, mm	6
Projectile material	Al6061
Projectile speed, km/s	7
Impact angle, degrees	0
Front facesheet thickness, mm	2
Rear facesheet thickness, mm	2
Facesheet material	Al6061-T6
Core thickness	40
Core material	Al6061-T6 Foam, 7.5% 40 PPI

Though both foam models (constant and stochastic) were made from the same material and foam wireframe with equivalent relative density, the morphological characteristics' distribution affects the intensity of shock waves generated in the foam and projectile which in turn affects the fragmentation process. Thus, the amount and the inherent nature of the fragments generated in the "Stochastic" foam would be probabilistic and much different from the generated within the "Constant" foam resulting in different outcome of HVI test on FCSP.

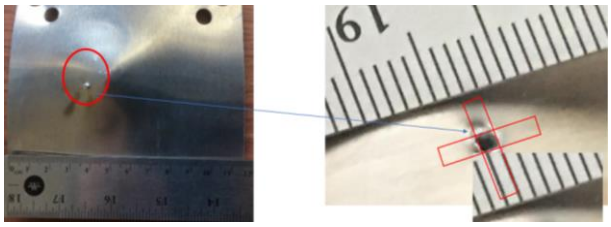

Figure 11. Damage of rear facesheet of FCSP specimen after physical HVI test (back view)

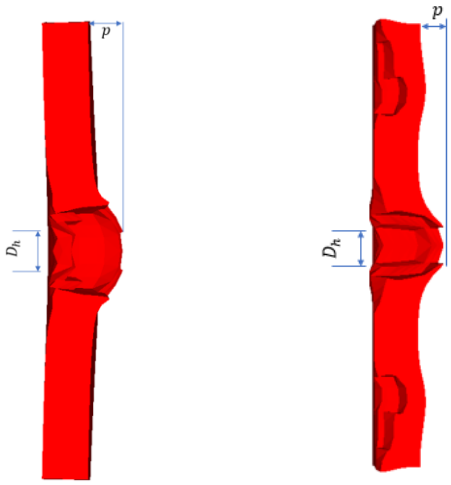

a) b)

Figure 12. Damage of rear FCSP facesheet after numerical HVI test: (a) "Constant" approach, e=1, t=17μs, D_h=1.78 mm and p=1.78; (b) "Stochastic" approach, e=1, t=17μs, D_h=1.38 mm and p=1.08

The "Stochastic" approach gives the predicted values of D_h=1.35 mm and p=1.08 vs experimentally obtained D_h=1.1-1.2 mm and p=1.3-1.4 mm. Therefore, the numerical analysis is rather conservative in comparison with the test data overestimating the perforation diameter and underestimating the rear wall bulge height.

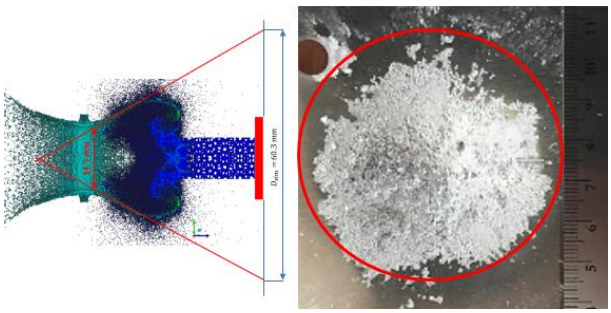

Figure 13. Debris cloud cone and damaged area on the rear facesheet

Another parameter that allows quantifying the simulation results is the cone angle of the debris cloud. For the performed simulation, this angle was equal 75.5º. The Fig. 13 demonstrates that the calculated value of the cone angle is consistent with the dimension of the damaged area on the rear facesheet (side adjacent to the foam) of the experimentally tested specimen.

The main stages of the foam-core panel penetration process are shown in Fig. 14. The simulation results illustrate that FCSP configuration can effectively cause projectile fragmentation providing a basis for a weight-efficient protection against MMOD particles.

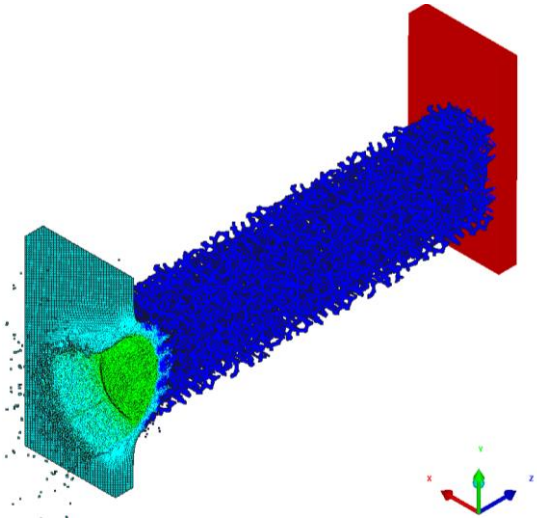

a) t=1 μs

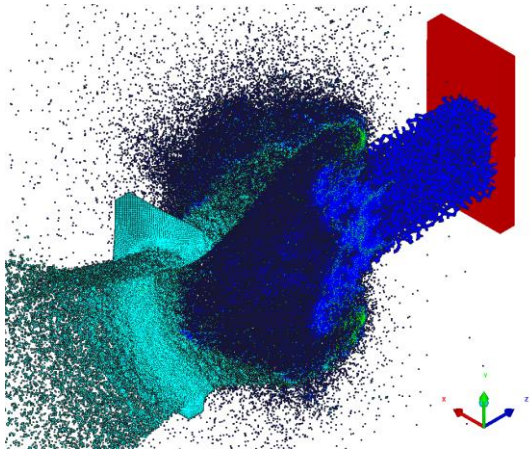

b) t=6 μs

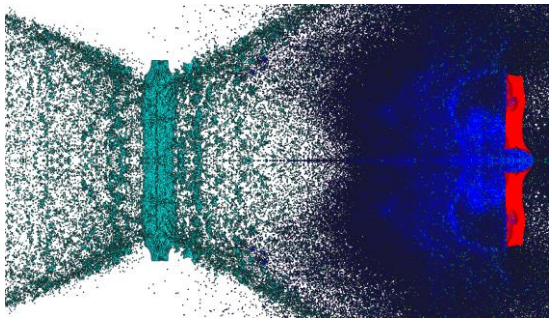

c) t=15 μs

Figure 14. Numerical simulation of HVI on FCSP

5 CONCLUSION

A highly detailed numerical model of foam-core sandwich panel subjected to MMOD impact is presented. Based on the foam sample analysis, the model foam was approximated by a combination of cylindrical ligaments and spherical nodes. Modelling procedure utilizes the enhanced randomization technique, which involves stochastic variations of nodes and ligaments dimensions, random perturbation of the node positions and rotation of the sub-units composing the foam geometry. The HVI simulations employed a combination of SPH and FEM in the Lagrangian formulation. The developed approach was evaluated by comparison of numerical and physical test outcomes for the FCSP specimens subjected to 6-mm spherical aluminum particle impact at 7 km/s. The developed model showed a good agreement with test data and can be used for the FCSP performance evaluation.

Acknowledgments

This work was supported by Magellan Aerospace Winnipeg and the Natural Sciences and Engineering Research Council of Canada (Discovery Grant no. 402115-2012).

6 REFERENCES

1. Ryan, S., Hedman, T., and Christiansen, E. L. (2010) Honeycomb vs. Foam: Evaluating a Potential Upgrade to ISS Module Shielding, *Acta Astronautica*, **67**(7-8), 818-825.
2. Yasensky J., Christiansen E. L. (2008) Hypervelocity impact evaluation of metal foam core sandwich structures, *NASA/TP-2008-214776*, NASA Johnson Space Center, Houston.
3. Destefanis, R., et al. (2003) Enhanced Space Debris Shields for Manned Spacecraft, *Int. J. Impact Eng.*, **29**(1-10), 215–226.
4. Destefanis, R., et al. (2006) Selecting Enhanced Space Debris Shields for Manned Spacecraft," *Int. J. Impact Eng*., **33**(1–12), 219–230.
5. Cherniaev, A., Telichev, I. (2017) Weight-Efficiency of Conventional Shielding Systems in Protecting Unmanned Spacecraft from Orbital Debris, *J. Spacecr. Rockets*, **54**(1), 75–89.
6. Okabe, A. et al. (2000) Spatial Tesselations: Concepts and Applications of Voronoi Diagrams. *Wiley Series in Probability and Statistics*, John Wiley & Sons Ltd.
7. Wejrzanowski, T. et al (2013) Structure of Foams Modeled by Laguerre-Voronoi Tessellations, *Comput. Mater. Sci.*, **67**, 216–221.
8. Lautensack, C. and Sych, T. (2006) 3D Image Analysis of Open Foams Using Random Tessellations, *Image Anal. Stereol*., **25**(2), pp. 87–93.
9. Helmut, J. (2006) Space-Filling Polyhedra as Mechanical Models for Solidified Dry Foams, Materials Transactions, **47**(9), 2213-2218.
10. Nie, Z., Lin, Y. and Tong, Q. (2017) Modeling structures of open cell foams, *Comput. Mater. Sci*., **131**(1), 160–169.
11. Zhu, H. X., Mills, N. J., and Knott, J. F. (1997) Analysis of the high strain compression of open-cell foams, *J. Mech. Phys. Solids*, **45**(11–12), 1875–1899.
12. Roberts, A. P., Garboczi, E. J. (2001) Elastic Moduli of Model Random Three-dimensional Closed-cell Cellular Solids, *Acta Mater*., **49**(2), 189–197.
13. Buffel, B. et al (2014) Modelling open cell-foams based on the Weaire – Phelan unit cell with a minimal surface energy approach, *Int. J. Solids Struct*., **51**, (19–20), 3461–3470.
14. Weaire, D., Phelan, R. (1994) A counter-example to kelvin's conjecture on minimal surfaces, *Philos. Mag. Lett.*, **69**(2), 107–110.
15. Roux, S. et al (2008) Three-dimensional Image Correlation from X-ray Computed Tomography of Solid Foam, *Composites Part A: Applied Science and Manufacturing*, **39**(8) pp. 1253–1265.
16. Miedzinska, D., Niezgoda, T. and Gieleta, R. (2012) Numerical and Experimental Aluminum Foam Microstructure Testing with the use of Computed Tomography, *Comput. Mater. Sci.*, **64**(Nov.), 90–95.
17. Jang, W., and Kyriakides, S. (2009) On the Crushing of Aluminum Open-Cell Foams : Part I . Experiments," *Int. J. Solids Struct.*, 46(3–4), 617–634.
18. Gong, L., Kyriakides, S. and Jang, W. (2005) Compressive Response of Open-cell Foams. Part I : Morphology and Elastic Properties, **42**, 1355–1379.